Fundamentals of Non-Local Total Variation Spectral Theory

Jean-François Aujol[1,2], Guy Gilboa[3(✉)], and Nicolas Papadakis[1,2]

[1] University of Bordeaux, IMB, UMR 5251, 33400 Talence, France
[2] CNRS, IMB, UMR 5251, 33400 Talence, France
[3] Electrical Engineering Department, Technion - IIT, Haifa, Israel
guy.gilboa@ee.technion.ac.il

Abstract. Eigenvalue analysis based on linear operators has been extensively used in signal and image processing to solve a variety of problems such as segmentation, dimensionality reduction and more. Recently, nonlinear spectral approaches, based on the total variation functional have been proposed. In this context, functions for which the nonlinear eigenvalue problem $\lambda u \in \partial J(u)$ admits solutions, are studied. When u is the characteristic function of a set A, then it is called a calibrable set. If $\lambda > 0$ is a solution of the above problem, then $1/\lambda$ can be interpreted as the scale of A. However, this notion of scale remains local, and it may not be adapted for non-local features. For this we introduce in this paper the definition of non-local scale related to the non-local total variation functional. In particular, we investigate sets that evolve with constant speed under the non-local total variation flow. We prove that non-local calibrable sets have this property. We propose an onion peel construction to build such sets. We eventually confirm our mathematical analysis with some simple numerical experiments.

Keywords: Non-local · Total variation · Calibrable sets · Scale · Nonlinear eigenvalue problem

1 Introduction

Since the seminal work by Rudin et al in [19], total variation is established as a main tool in mathematical image processing. It has been used for many applications such as denoising, deblurring, inpainting (see e.g. [3] and references herein). In a series of papers, V. Caselles and his co-authors have computed explicit solutions of the total variation flow problem [1,2,9]:

$$\begin{cases} u(x,0) = f(x), \\ \frac{\partial u}{\partial t} \quad = \operatorname{div}\left(\frac{\nabla u}{|\nabla u|}\right). \end{cases} \tag{1}$$

In particular, it is shown that if $f = \chi_A$ with A a non empty closed convex set, such that the absolute value of its curvature is smaller than $\lambda_A = \frac{\mathrm{Per}(A)}{|A|}$ (with $\mathrm{Per}(A)$ the perimeter of A and $|A|$ its area) , then the solution of (1) is given by

J.-F. Aujol et al. (Eds.): SSVM 2015, LNCS 9087, pp. 66–77, 2015.
DOI: 10.1007/978-3-319-18461-6_6

$u(t) = (1 - t\lambda_A)^+ \chi_A$. More generally, calibrable sets evolve with constant speed under the total variation flow. Notice that the notion of calibrable sets was also a key ingredient to build explicit solutions of the $TV - L^1$ problem [10,11]. The quantity $\lambda_A = \frac{\mathrm{Per}(A)}{|A|}$, known as the Cheeger constant, can be seen as the inverse of a scale, and this has been used in works such as [7,15,20,21].

A calibrable set A is such that the following nonlinear eigenvalue problem has a solution (with $u = \chi_A$):

$$p(u) = \lambda u, \ p(u) \in \partial J(u), \tag{2}$$

where $J(u)$ is the total variation functional and $\partial J(u)$ is its subgradient.

In [13] a generalization of eigenfunction analysis to the nonlinear case was proposed in the following way. Define

$$\phi(t; x) := u_{tt}(t; x)t, \tag{3}$$

where u_{tt} is the second time derivative of the solution $u(t; x)$ of the TV-flow (1). For $f(x)$ admitting (2), with a corresponding eigenvalue λ, one obtains $\phi(t; x) = \delta(t - 1/\lambda)f(x)$. When f is composed of separable eigenfunctions with eigenvalues λ_i one obtains through $\phi(t; x)$ a decomposition of the image into its eigenfunctions at $t = 1/\lambda_i$. In the general case, ϕ yields a continuum multi-scale representation of the image, generalizing structure-texture decomposition methods like [4,5,17]. One can reconstruct the original image by:

$$f(x) = \int_0^\infty \phi(t; x)dt + \bar{f}, \tag{4}$$

where $\bar{f} = \frac{1}{|\Omega|} \int_\Omega f(x)dx$. Given a transfer function $H(t) \in \mathbb{R}$, image filtering can be performed by:

$$f_H(x) := \int_0^\infty H(t)\phi(t; x)dt + \bar{f}.$$

The spectrum $S(t)$ corresponds to the amplitude of each scale:

$$S(t) := \|\phi(t; x)\|_{L^1(\Omega)} = \int_\Omega |\phi(t; x)|dx. \tag{5}$$

The goal of this paper is to extend this notion of scale to a non-local setting. Non-local approaches have become very popular in the last past years since the seminal work by Buades et al [8]. A non-local version of the total variation based on graphs was introduced in [14]. See recent related studies analyzing non-local and double-integral functionals in [6,18]. Here we intend to propose a non-local notion of scale, and to this end we will introduce a notion of non-local disks and more generally of non-local calibrable sets.

The plan of the paper in the following. In section 2, we recall the non-local setting introduced in [14], and how it connects to the classical local setting. In section 3, we consider the graph point of view of [12,22] to define all the non-local notions we need, and in particular a non-local scale. In section 4, we propose a construction of non-local disks based on an onion peel analysis. We eventually show some numerical results to illustrate our analysis in Section 5.

2 Background and Definitions of Non-Local Operators

We first recall the basic non-local operators. We give the definitions in the continuous setting in order to make clear connections with respect to the classical local variational approaches.

2.1 Non-Local Operators

Given a bounded domain $\Omega \subset \mathbb{R}^2$ we have non-negative weights $w(x,y) \geq 0$ between any two points $x, y \in \Omega$. These weights correspond to affinities between the points. For simplicity, we assume that the weights are symmetric, that is $w(x,y) = w(y,x)$, the extension to non symmetric weights being straightforward. In this context we have two types of functions: scalar functions and vector functions. Scalars are the standard functions $u : \Omega \to \mathbb{R}$, whereas vectors, denoted $\boldsymbol{v}(x)$, or $v(x,y)$, have the following mapping $v : \Omega \times \Omega \to \mathbb{R}$. For example, a non-local gradient maps a scalar to a vector function.

The inner product of two vectors $\boldsymbol{v}_1(x)$ and $\boldsymbol{v}_2(x)$ is defined as:

$$\langle \boldsymbol{v}_1, \boldsymbol{v}_2 \rangle_\Omega := \int_\Omega v_1(x,y) v_2(x,y) dy. \tag{6}$$

We can now define the main non-local operators. The non-local gradient $\nabla_w u(x)$: $\Omega \to \Omega \times \Omega$ is defined as:

$$(\nabla_w u)(x,y) := (u(y) - u(x)) \sqrt{w(x,y)}, \quad x, y \in \Omega. \tag{7}$$

The non-local divergence $\mathrm{div}_w\, \boldsymbol{v}(x) : \Omega \times \Omega \to \Omega$ is:

$$(\mathrm{div}_w\, \boldsymbol{v})(x) := \int_\Omega (v(x,y) - v(y,x)) \sqrt{w(x,y)} dy. \tag{8}$$

Some basic properties, similar to the standard local operators, can be shown, as for example the gradient and divergence adjoint relation:

$$\langle \nabla_w u, \boldsymbol{v} \rangle = \langle u, -\mathrm{div}_w\, \boldsymbol{v} \rangle. \tag{9}$$

2.2 Non-Local Total-Variation

The difference-based functional we consider is

$$J(u) = \int_{\Omega \times \Omega} \psi((u(y) - u(x))^2 w(x,y)) dy dx, \tag{10}$$

and its variation with respect to u reads

$$\partial_u J(u) = -4 \int_\Omega (u(y) - u(x)) w(x,y) \psi'((u(y) - u(x))^2 w(x,y)) dy. \tag{11}$$

Taking $\psi(s) = \sqrt{s}/2$ we define the non-local total-variation as:

$$J_{NL-TV}(u) = \frac{1}{2} \int_{\Omega \times \Omega} |u(x) - u(y)| \sqrt{w(x,y)} dy dx \tag{12}$$

The above functional corresponds in the local two dimensional case to the anisotropic TV:

$$J_{TV}(u) = \int_{\Omega} (|u_{x_1}| + |u_{x_2}|)dx.$$

Although all the results of the paper remain true in the isotropic case, we have decided to present in this work only the anisotropic setting. Following the clocal TV-flow [16], we are investigating the non-local total variation flow (NL-TV-flow):

$$\begin{cases} -\frac{\partial u}{\partial t} \in \partial_u J_{NL-TV}(u) \\ u(0,x) = f(x) \end{cases} \tag{13}$$

Now that we have recalled the non-local notions we are interested in, we turn in the next section to a graph setting which will prove more adapted to the non-local framework.

3 A Graph Point of View

As soon as we consider a discrete image, the connections between pixels can be explained with a graph representation. We will place ourselves in this setting from now on.

3.1 Definitions

We consider a graph $\mathcal{G}$ (which corresponds to the bounded domain Ω considered in the previous section). It is composed of $|\mathcal{G}|$ points $x \in \mathcal{G}$ and characterized by the adjacency matrix $w(x,y) : \mathcal{G} \times \mathcal{G} \to \in [0;1]^{|\mathcal{G}|}$. We assume that this matrix is symmetric. Notice that this adjacency matrix corresponds to the non negative weights $w(x,y)$ introduced in the previous section. We have decided to use the same notation for the sake of clarity.

Definition 1 (Boundary of a set). *The intern boundary of a set A is defined as:*

$$\partial A = \{x \in A,\ s.t\, \exists\, y \in \mathcal{G} \backslash A,\ with\, w(x,y) > 0\}.$$

The extern boundary of a set A is defined as:

$$\partial A^{+} = \{x \in \mathcal{G} \backslash A,\ s.t\, \exists\, y \in A,\ with\, w(x,y) > 0\}.$$

Let χ_A be a characteristic function of $A \subset \mathcal{G}$. We remind the reader that $\chi_A(x) = 1$ if $x \in A$ and 0 otherwise.

Definition 2 (Perimeter of a set).
The perimeter of a set A is defined as:

$$Per_w(A) = J_{NL-TV}(\chi_A) = \frac{1}{2} \sum_{\mathcal{G} \times \mathcal{G}} |\chi_A(x) - \chi_A(y)| \sqrt{w(x,y)} \tag{14}$$

Definition 3 (Normal of a set). *The normal of a set A is defined on its boundary $x \in \partial A$ as, for $y \in \partial A^+$: $\nu_A(x,y) = -sgn(\nabla_w \chi_A(x,y)) = \chi_{w(x,y)>0}$. The minus is a convention. Observe that $Per_w(A) = -\langle \nu_A^a, \nabla_w \chi_A \rangle_{\mathcal{G}\times\mathcal{G}}$.*

Definition 4 (Curvature of a set). *The curvature of a set $A \subset \mathcal{G}$ is*

$$\kappa_w(\chi_A)(x) = \mathrm{div}_w(-sgn(\nabla_w \chi_A(x,y))) \tag{15}$$

We assume that the domain $\mathcal{G}$, the set A and its complement $\mathcal{G}\backslash A$ are all connected sets.

3.2 Sets With Constant Curvature

Now that we have introduced the necessary material, we can characterize the sets with constant curvatures. Notice that in the classical local setting, these sets are just balls (whose shape depends on the considered norm). As we will see in the following, we get a necessary and sufficient condition to characterize sets with constant curvature. Sets with constant curvature will be key ingredients to introduce non-local calibrable sets.

Proposition 1. *A necessary and sufficient condition for $\kappa_w(\chi_A)(x)|_{x\in\partial A} = K \in \mathbb{R}$ is:*

$$\sum_{y\in\partial A^+} \sqrt{w(x,y)} = a^+ \in \mathbb{R}^+, \forall x \in \partial A.$$

The curvature value at the boundary ∂A is $K = 2a^+$.

Proof. We can use the definition (15) of the mean curvature for χ_A, the characteristic function of $A \subset \mathcal{G}$. For $x \in \partial A$, as $w(x,y) = 0$, $\forall y \in \mathcal{G}\backslash(A \cup \partial A^+)$ we get:

$$\begin{aligned}
\kappa_w(\chi_A)(x) =& -\sum_{y\in\mathcal{G}} \left(\mathrm{sgn}\left((\chi_A(y) - \chi_A(x))w_{xy}\right) - \mathrm{sgn}\left((\chi_A(x) - \chi_A(y))w_{xy}\right)\right) w_{xy} \\
=& -\sum_{y\in A\cup\partial A^+} \left(\mathrm{sgn}\left((\chi_A(y) - 1)w_{xy}\right) - \mathrm{sgn}\left((1 - \chi_A(y))w_{xy}\right)\right) w_{xy} \\
=& -\sum_{y\in A} \left(\mathrm{sgn}(0) - \mathrm{sgn}(0)\right) w_{xy}\, dy + \sum_{\partial A^+} \left(\mathrm{sgn}(-w_{xy}) - \mathrm{sgn}(w_{xy})\right) w_{xy} \\
=& 2 \sum_{y\in\partial A^+} w_{xy},
\end{aligned}$$

since $w_{xy} = \sqrt{w(x,y)} \geq 0$. A necessary and sufficient condition for $\kappa_w(\chi_A)(x)|_{x\in\partial A} = 2a^+ \in \mathbb{R}^+$ is then

$$\sum_{y\in\partial A^+} \sqrt{w(x,y)} = a^+ \in \mathbb{R}^+, \forall x \in \partial A.$$

In the same way, we get:

$$\kappa_w(\chi_A)(x) = \begin{cases} 2a^+ & if\, x \in \partial A \\ 0 & if\, x \in A \backslash \partial A \\ -2a^- & if\, x \in \partial A^+ \\ 0 & if\, x \in \mathcal{G} \backslash (A \cup \partial A^+), \end{cases} \tag{16}$$

under the assumption $\sum_{y \in \partial A} \sqrt{w(x,y)} = a^- \in \mathbb{R}^+, \forall x \in \partial A^+$.

From the last proposition, the curvature is constant iff:

- for $x \in \partial A$, $\sum_{y \in \partial A^+} \sqrt{w(x,y)} = a^+ > 0$
- for $x \in \partial A^+$, $\sum_{y \in \partial A} \sqrt{w(x,y)} = a^- > 0$

A set with constant curvature in its intern and extern boundaries is then characterized with the parameters (a^+, a^-).

Proposition 2 (Sets with constant curvature). *When the intern and extern curvature sof a set A are constants with parameters (a^+, a^-), the perimeter reads:*

$$Per_w(A) = \frac{1}{2}(|\partial A| a^+ + |\partial A^+| a^-) = |\partial A| a^+.$$

Proof. We have:

$$\begin{aligned} \mathrm{Per}_w(A) &= \frac{1}{2} \sum_{\mathcal{G} \times \mathcal{G}} |\chi_A(x) - \chi_A(y)| \sqrt{w(x,y)} \\ &= \frac{1}{2} \sum_{x \in \partial A,\, y \in \mathcal{G}} |\chi_A(x) - \chi_A(y)| \sqrt{w(x,y)} + \frac{1}{2} \sum_{x \in \partial A^+,\, y \in \mathcal{G}} |\chi_A(x) - \chi_A(y)| \sqrt{w(x,y)} \\ &= \frac{1}{2}(|\partial A| a^+ + |\partial A^+| a^-) \end{aligned}$$

and as w is symmetric, we have that the total weights a^+ going from ∂A to ∂A^+ is the same than the weights a^- going from ∂A^+ to ∂A: $|\partial A| a^+ = \sum_{x \in \partial A,\, y \in \mathcal{G}} |\chi_A(x) - \chi_A(y)| \sqrt{w(x,y)} = \sum_{x \in \partial A^+,\, y \in \mathcal{G}} |\chi_A(x) - \chi_A(y)| \sqrt{w(x,y)} = |\partial A^+| a^-$.

3.3 Subdifferential of J_{NL-TV}

Another ingredient needed to introduce non-local calibrable sets is the subdifferential of non-local TV. As recalled in [22], the subdifferential of $NL-TV$ is characterized by:

$$\partial J_{NL-TV}(u) = \{\mathrm{div}_w(z) \;/\; \max |z| \leq 1 \text{ and } \langle \mathrm{div}_w z, u \rangle_{\mathcal{G}} = J_{NL-TV}(u)\} \tag{17}$$

Denoting $z = -sign(\nabla_w u)$, with $sign(0) \in [-1, 1]$, the subdifferential of J_{NL-TV} is:

$$\partial J_{NL-TV}(u) = \mathrm{div}_w(z). \tag{18}$$

From Definition 3, it can be noticed that

$$\partial J_{NL-TV}(\chi_A) = \mathrm{div}_w(\nu_A). \tag{19}$$

3.4 Non-Local Calibrable Sets

We have all the required material to define non-local calibrable sets. As we will see later, such sets evolve with constant speed with the non-local total variation flow.

Definition 5 (Non-local calibrable set). *A is a non-local calibrable set iff there exists $\lambda_A > 0$ and $\mathrm{div}_w(z) \in \partial J_{NL-TV}(\chi_A)$ such that $(\mathrm{div}_w z)(x) = \lambda_A \chi_A(x) + c$, $\forall x \in A$, $\quad c \in \mathbb{R}$. Such z is called a calibration of the set A.*

Remark 1. Notice that contrary to the continuous local case (see e.g. [1]), there are no boundary conditions such as Neuman boundary conditions. We have these boundary conditions for free here since the non-local divergence operator was defined as the opposite of the adjoint of the non-local gradient operator. Moreover, as noted in [22], the value of the divergence outside A is irrelevant, so that we just focus on finding a flow with constant divergence inside A.

Proposition 3. *If z is a calibration of a non-local set A, then*

$$(\mathrm{div}_w z)(x) = \frac{Per_w(A)}{|A|}\chi_A \tag{20}$$

and thus $\lambda_A = \frac{Per_w(A)}{|A|}$. Moreover, $z(x,y) = \nu_A(x,y)$ for $x \in \partial A$, $y \in \partial A^+$.

Proof. From Definition 5, we can observe that $\langle \mathrm{div}_w z, \chi_A \rangle_{\mathcal{G}} = \lambda_A |A|$. Hence, as $z \in \partial J_{NL-TV}(\chi_A)$, relation (17) gives $\langle \mathrm{div}_w z, \chi_A \rangle_{\mathcal{G}} = J_{NL-TV}(\chi_A) = \mathrm{Per}_w(A)$ so that $\lambda_A = \frac{\mathrm{Per}_w(A)}{|A|}$.

Moreover, from Definition 3, we have that $\mathrm{Per}_w(A) = -\langle \nu_A, \nabla_w \chi_A \rangle$. Since $\langle \mathrm{div}_w z, \chi_A \rangle_{\mathcal{G}} = -\langle z, \nabla_w \chi_A \rangle_{\mathcal{G}\times\mathcal{G}}$, we deduce that $z(x,y) = \nu_A(x,y)$ for $x \in \partial A$, $y \in \partial A^+$.

3.5 Non-Local TV Flow

For a set $A \in \mathcal{G}$, the non-local TV flow evolution equation is Eq. (13) with $u(t=0) = \chi_A$.

Proposition 4. *If A is a non-local calibrable set, then $u(t) = (1 - t\lambda_A)^+ \chi_A$ is a solution of Problem (13), with $\lambda_A = \frac{Per_w(A)}{|A|}$.*

We remind the reader that $(1 - t\lambda_A)^+ = \max(0, 1 - t\lambda_A)$. This result shows that a non-local calibrable set evolves with constant speed with the non-local total variation flow. We know that such sets exist (and the onion peel story of section 4 is a way to build such sets).

Proof. With the above results, if A is a non-local calibrable set, then we can build a flow z such that $||z||_\infty \leq 1$, $z = \nu_A$ on $\partial A \cup \partial A^+$ and $(\mathrm{div}_w z)(x) = \lambda_A$ for $x \in A$. We therefore have $\langle \mathrm{div}_w z, \chi_A \rangle_{\mathcal{G}} = \lambda_A |A| = \mathrm{Per}_w(A) = J_{NL-TV}(\chi_A)$. From the definition (17) of the NL-TV functional, we also have $J_{NL-TV}(u) = \sup_{||z||_\infty \leq 1} \int_{\Omega\times\Omega} (\mathrm{div}_w z) u$.

We can see that the z we built is such that $\mathrm{div}_w z$ belongs to the subdifferential of J_{NL-TV} so that $(\mathrm{div}_w z)(x) = \lambda_A$ for $x \in A$. Hence, by defining $u(t) = (1 - t\lambda_A)^+ \chi_A$, we have for $t > 0$ that $\partial_t u = -\lambda_A \chi_A$ so that $-\partial_t u \in J_{NL-TV}(u)$ and u is a solution of problem (13).

3.6 Non-Local Scale

From the previous proposition, it makes sense to define the non-local scale in the following way:

Definition 6 (Non-local scale). *The non-local scale of a point in an image is defined as the inverse of its average speed of decrease under the non-local total variation flow.*

Remark 2. In the case when a point x belongs to a non-local disk A, then its speed of decrease under the non-local total variation flow is the one of A, that is $\lambda_A = \frac{\mathrm{Per}_w(A)}{|A|}$. Hence the scale of x is $\frac{1}{\lambda_A}$. This generalizes the local case, where λ_A is the Cheeger constant of A [2,11].

4 The Onion Peel Decomposition

The purpose of this section is to show a way to build non trivial non-local calibrable sets. In the following, we denote as $\{B_r\}_{r=1}^R$ a partition of A ($\cup_{r=1}^R B_r = A$ and $B_r \cap B_{r'} = \emptyset$, for $r \neq r'$) and define $A_r = \cup_{i=1}^r B_i$. The idea developed here is inspired from the local discrete case: if we remove the boundary of a calibrable set, the resulting set is also calibrable.

Definition 7 (Onion peel partition). *Let A be a connected set. We say that A can be partitioned into onion peels if there exists a partition that checks:*

(i) $\partial A_r = B_r$, $\forall r = 1 \cdots R$.
(ii) $\partial A_r^+ = B_{r+1}$, $\forall r = 1 \cdots R-1$

We then have $\partial A = B_R$ since $A = A_R$.

Definition 8 (Non-local Disk). *A is a non-local disk iff A is a non-local calibrable set with constant curvature on ∂A.*

Proposition 5 (Calibrable onion peel). *If (i) A can be partitioned into an onion peel $\{B_r\}_{r=0}^R$, (ii) $A_r = \cup_{i=0}^r B_i$ has a constant curvature (a_r^+, a_r^-) and (iii) $A = A_R = \underset{r}{argmin}\ Per_w(A_r)/|A_r|$, then A is a non-local disk, and its non-local scale is $\frac{|A|}{Per_w(A)}$.*

Proof. We build a calibration z for an onion peel. By definition of the onion peel, we first recall that for $x \in B_r$, $w(x,y) = w(y,x) > 0$ iff $y \in B_{r-1}$ or $y \in B_r$ or $y \in B_{r+1}$. From proposition 2, we can observe that $a_r^+ |B_r| = a_r^- |B_{r+1}|$ and $\mathrm{Per}_w(A_r) = \frac{1}{2}(|\partial A_r| a_r^+ + |\partial A_r^+| a_r^-) = |\partial A_r| a_r^+$. We recall that a_r^- denotes the constant curvature value of points ∂A_r^+ with respect to the set A_r.

We define $K_0 = 0$, $a_0^- = 0$, initialize $z = 0$ and consider a value $\alpha > 0$. Then for $r = 1 \cdots R$ we can do the following recursive construction: $\forall x \in B_r$, find the $y \in B_{r+1}$ such that $w(x,y) > 0$ and set $z(x,y) = K_r = \frac{a_{r-1}^- K_{r-1} + \alpha}{a_r^+}$. We then have $z(x,y) = K_r > 0$ for $x \in B_r$, $y \in B_{r+1}$ and $w(x,y) > 0$ and $z = 0$ otherwise. With such a construction, we have that, for $x \in B_r$, $0 \leq r \leq R$:

$$\begin{aligned}
(\mathrm{div}_w\, z)(x) &= \sum_y (z(x,y) - z(y,x))\sqrt{w(x,y)} \\
&= \sum_{y \in B_{r+1}} z(x,y)\sqrt{w(x,y)} - \sum_{y \in B_{r-1}} z(y,x)\sqrt{w(x,y)} \\
&= K_r \sum_{y \in B_{r+1}} \sqrt{w(x,y)}dy - K_{r-1} \sum_{y \in B_{r-1}} \sqrt{w(x,y)}dy \\
&= \frac{a_{r-1}^- K_{r-1} + \alpha}{a_r^+} a_r^+ - K_{r-1} a_{r-1}^- \\
&= \alpha,
\end{aligned}$$

For $x \in A$, we have that $||z(x)||_\infty \leq \max_r K_r = K^*$. We then obtain that $||z(x)/K^*||_\infty \leq 1$ and $(\mathrm{div}_w\, z/K^*)(x) = \alpha/K^*$, for $x \in A$.

Next, with our assumption on the constant curvature of the onion peel partition (see Definitions 7 and 5) , we know that: $a_r^+|B_r| = a_r^-|B_{r+1}|$: the total weights a_r^+ going from B_r to B_{r+1} is the same as the weights a_r^- going from B_{r+1} to B_r. Since $K_1 = \alpha/a_1^+$, we have that

$$K_2 = \frac{a_1^- K_1 + \alpha}{a_1^+} = \frac{a_1^- \alpha/a_1^+ + \alpha}{a_2^+} = \frac{\alpha}{a_2^+}\left(1 + \frac{|B_1|}{|B_2|}\right) = \frac{\alpha(|B_1| + |B_2|)}{a_2^+|B_2|}$$

We can prove by induction that for $r = 1 \cdots R$:

$$K_r = \frac{\alpha \sum_{i=0}^r |B_i|}{a_r^+|B_r|} = \frac{\alpha|A_r|}{a_r^+|\partial A_r|} = \frac{\alpha|A_r|}{\mathrm{Per}_w(A_r)}$$

Hence, $K^* = \max_r K_r = \alpha/\lambda_A$ where

$$\lambda_A = \min_{A_r \subset A} \frac{\mathrm{Per}_w(A_r)}{|A_r|}.$$

We then have that, for $x \in A$, $(\mathrm{div}_w\, z/K^*)(x) = \alpha/K^* = \lambda_A$. Hence: $\langle \mathrm{div}_w\, z, \chi_A \rangle = \lambda_A|A|$. If $A = A_R = \mathrm{arg}min_r \mathrm{Per}_w(A_r)/|A_r|$, then $K^* = K_R$. We thus obtain that $||z(x,y)/K^*|| = 1$ for $x \in \partial A$, $y \in \partial A^+$ and $w(x,y) > 0$ so that the flow corresponds to the normal of the set at these points: $z(x,y) = \nu_A(x,y)$ (see Definition 3) and A is a non-local disk from definition 8. In this case, it also means that $\langle \mathrm{div}_w\, z, \chi_A \rangle = \lambda_A|A| = \mathrm{Per}_w(A)$.

Remark 3. Notice that since $K_r = \frac{a_{r-1}^- K_{r-1} + \alpha}{a_r^+}$, then a sufficient condition to have a disk through $K^* = K_R$ is $a_{r-1}^- \geq a_r^+$, which means that for each $x \in B_r$ the total weights of its links with B_{r-1} is larger than with B_{r+1}. With respect to the aniotropic local case and a 4-neighborhood system with weights $w(x,y) \in \{0;1\}$, such property is trivially checked since $a_r^+ = a_r^- = 2$.

5 Numerical Experiments

In this section, we show some simple numerical experiments which confirm the theoretical results presented in the previous sections. We consider synthetic images representing the characteristic function of some objects and build two graphs. First, we consider a local graph corresponding to a 4 neighborhood system to compute the anisotropic TV flow. The local adjacency matrix thus reads $w^L(x,y) = 1$ if x and y are neighbors in the image domain and 0 otherwise. Then, a full non-local graph is built from self-similarities between patches centered on every pixels of a considered image f. The adjacency matrix is in this case defined as: $w^{NL}(x,y) = exp(-||P_x^f - P_y^f||^2)$, where P_x^f denotes the image patch centered on pixel x. This corresponds to a non-local mean graph construction for the image f. The non-local TV flow (13) is then applied to the synthetic images for the two graph settings giving us two sequences $u^L(t,x)$ and $u^{NL}(t,x)$. We then compute the NL-TV spectral transform $\phi(t,x)$ and spectrum $S(t)$ as in Eqs. (3) and (5), respectively, with $u(t,x)$ the NL-TV flow solution of (13). High amplitudes in $S(t)$ indicate the dominant scales contained in the image. Notice that the non-local TV flow, derived from the the local graph with weights w^L, is in fact the classical TV flow. In our illustrations, we considered two objects of different scales for each tested image. As illustrated in Fig. 1, in the local setting, each object has a different scale, since two main peaks appear in $S^L(t)$. On the other hand, with the non-local weights, the two objects are considered as a single one as $S^{NL}(t)$ only contains one peak.

In the first row of Fig. 1, the objects are squares so that they correspond to a disk for the local anisotropic TV flow. As the local anisotropic Cheeger constants of the two squares are $8/3$ and $4/3$, we see from proposition 4 that the objects vanish with the TV flow for $t = 3/8$ and $t = 3/4$, which correspond to the positions of the two peaks of $S^L(t)$. With the non-local graph represented by w^{NL}, the non-local scale of the union of the two squares can thus be deduced from $S^{NL}(t)$ where the most important peak is at time $t = 0.015$. As the non-local curvature of the shape is not constant, we nevertheless observe a spread peak and the union of the two squares is just a raw approximation of a non-local calibrable set for the graph w^{NL}.

In the second row, the example is composed of non-rectangular shapes, the objects are not calibrable sets anymore for the local graph w^L. This is exhibited by the spread peaks of $S^L(t)$. It is difficult to assess the presence of two objects with the local framework since $S^L(t)$ contains 4 peaks. With the full non-local graph, one peak is recovered and its non-local scale is almost the same as in the square example. The non-local curvature is here almost constant so that we recover a main peak. This shows that these objects approach non-local calibrable sets for the graph w^{NL}.

These results give an interesting point of view of the non-local means behaviour. When constructing a graph with respect to the similarities contained in an image and applying the NL-TV flow to this image, one can expect that groups of similar patterns will have a constant speed of decrease.

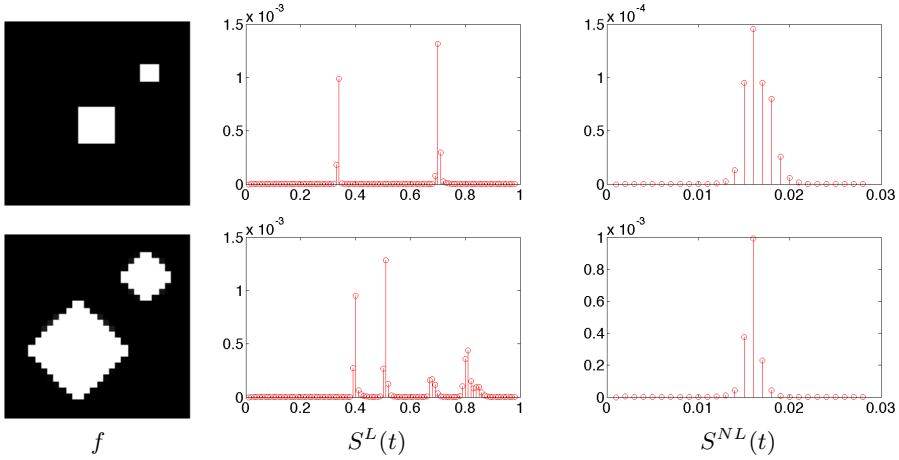

Fig. 1. Examples of scale computation. First column: images f; second column: local scale $S^L(t)$; third column: non-local scale $S^{NL}(t)$. The non-local scale gives indeed the same scale to the two shapes, whereas the local version give two different scales and even badly characterize the 2 objects for the second row.

6 Conclusion

The paper formulates a platform for spectral analysis related to the non-local total variation functional. Non-local calibrable sets, which are nonlinear eigenfunctions in the sense of (2), or atoms of the functional, are defined. A constructive way to build a subset of them is given. New structures such as non-local disks are examined through this framework, extending the standard geometrical concepts. The framework is a first step toward a better analysis and design of non-local, image-driven and patch-based algorithms, which have shown to yield state-of-the-art results in image processing and computer vision in recent years.

Acknowledgments. This study has been carried out with financial support from the French State, managed by the French National Research Agency (ANR) in the frame of the Investments for the future Programme IdEx Bordeaux (ANR-10-IDEX-03-02). J-F. Aujol acknowledges the support of Institut Universitaire de France. G. Gilboa acknowledges the support of the Mallat Family Fund.

References

1. Andreu, F., Ballester, C., Caselles, V., Mazon, J.M.: Minimizing total variation flow. Differential and Integral Equations **14**(3), 321–360 (2001)
2. Andreu-Vaillo, F., Caselles, V., Mazon, J.M.: Parabolic quasilinear equations minimizing linear growth functionals. Progress in Mathematics, vol. 223. Birkhauser (2002)
3. Aubert, G., Kornprobst, P.: Mathematical Problems in Image Processing. Applied Mathematical Sciences, vol. 147. Springer (2002)

4. Aujol, J.-F., Gilboa, G., Chan, T., Osher, S.: Structure-texture image decomposition - modeling, algorithms, and parameter selection. International Journal of Computer Vision **67**(1), 111–136 (2006)
5. Aujol, J.F., Aubert, G., Blanc-Féraud, L., Chambolle, A.: Image decomposition into a bounded variation component and an oscillating component. Journal of Mathematical Imaging and Vision **22**(1), 71–88 (2005)
6. Boulanger, J., Elbau, P., Pontow, C., Scherzer, O.: Non-local functionals for imaging. In: Fixed-Point Algorithms for Inverse Problems in Science and Engineering, pp. 131–154. Springer (2011)
7. Brox, T., Weickert, J.: A tv flow based local scale measure for texture discrimination. In: Pajdla, T., Matas, J.G. (eds.) ECCV 2004. LNCS, vol. 3022, pp. 578–590. Springer, Heidelberg (2004)
8. Buades, A., Coll, B., Morel, J.M.: A review of image denoising algorithms, with a new one. Multiscale Modeling and Simulation (SIAM Interdisciplinary Journal) **4**, 490–530 (2005)
9. Caselles, V., Chambolle, A., Moll, S., Novaga, M.: A characterization of convex calibrable sets in $\mathbb{R}^n$ with respect to anisotropic norms. Annales de l'Institut Henri Poincaré **25**, 803–832 (2008)
10. Chan, T.F., Esedoglu, S.: Aspects of total variation regularized L^1 function approximation. SIAM Journal on Applied Mathematics **65**(5), 1817–1837 (2005)
11. Duval, V., Aujol, J.-F., Gousseau, Y.: The tvl1 model: a geometric point of view. SIAM Journal on Multiscale Modeling and Simulation **8**(1), 154–189 (2009)
12. Elmoataz, A., Lezoray, O., Bougleux, S.: Nonlocal discrete regularization on weighted graphs: A framework for image and manifold processing. IEEE Transactions on Image Processing **17**(7), 1047–1060 (2008)
13. Gilboa, G.: A total variation spectral framework for scale and texture analysis. SIAM Journal on Imaging Sciences **7**(4), 1937–1961 (2014)
14. Gilboa, G., Osher, S.: Nonlocal operators with applications to image processing. SIAM Multiscale Modeling and Simulation **7**(3), 1005–1028 (2008)
15. Luo, B., Aujol, J.-F., Gousseau, Y.: Local scale measure from the topographic map and application to remote sensing images. SIAM Journal on Multiscale Modeling and Simulation (in press 2009)
16. Moll, J.S.: The anisotropic total variation flow. Mathematische Annalen **332**, 177–218 (2005)
17. Osher, S.J., Sole, A., Vese, L.A.: Image decomposition and restoration using total variation minimization and the H^{-1} norm. Multiscale Modeling and Simulation: A SIAM Interdisciplinary Journal **1**(3), 349–370 (2003)
18. Pontow, C., Scherzer, O.: Analytical Evaluations of Double Integral Expressions Related to Total Variation. Springer (2012)
19. Rudin, L., Osher, S., Fatemi, E.: Nonlinear total variation based noise removal algorithms. Physica D **60**, 259–268 (1992)
20. Strong, D., Aujol, J.-F., Chan, T.F.: Scale recognition, regularization parameter selection, and Meyer's G norm in total variation regularization. SIAM Journal on Multiscale Modeling and Simulation **5**(1), 273–303 (2006)
21. Strong, D., Chan, T.: Edge-preserving and scale-dependent properties of total variation regularization. Inverse Problems **19**(6), 165–187 (2003)
22. van Gennip, Y., Guillen, N., Osting, B., Bertozzi, A.L.: Mean curvature, threshold dynamics, and phase field theory on finite graphs. Milan Journal of Mathematics **82**(1), 3–65 (2014)